ELSEVIER

Biochimica et Biophysica Acta 1559 (2002) 160–170

BIOCHIMICA ET BIOPHYSICA ACTA
BBA

www.bba-direct.com

Translocation of protegrin I through phospholipid membranes: role of peptide folding

Guillaume Drin [a,b,*], Jamal Temsamani [a]

[a] *Synt:em, Parc Scientifique Georges Besse, 30000 Nîmes, France*
[b] *Centre de Biochimie Structurale, Faculté de Pharmacie, 15 Avenue Charles Flahault, 34060 Montpellier Cedex, France*

Received 26 July 2001; received in revised form 9 November 2001; accepted 22 November 2001

Abstract

The protegrin PG-1, belonging to the family of β-stranded antimicrobial peptides, exerts its activity by forming pores in the target biological membranes. Linear analogues derived from PG-1 do not form pores in the phospholipid membranes and have been used successfully to deliver therapeutic compounds into eucaryotic cells. In this paper, the translocation of PG-1 and of a linear analogue through artificial phospholipid membranes was investigated, leading to a possible mechanism for the activity of these peptidic vectors. We report here that [12W]PG-1, a fluorescent analogue of PG-1, is able to translocate through lipid bilayers and we demonstrate that this property depends on its secondary structure. Our results agree with the recent mechanism proposed for the translocation and permeabilisation activities of several helical and β-stranded peptides. In addition, our data corroborate recent work suggesting that certain protegrin-derived vectors enter into endothelial cells by adsorptive-mediated endocytosis.

Keywords: Peptide–lipid interaction; Protegrin; Translocation; Fluorescence; Peptidic vector

1. Introduction

Protegrin-1 (PG-I) is an 18-amino-acid peptide isolated originally from porcine leucocyte cells [1]. This peptide displays a broad-range antimicrobial activity spectrum [1–3] and has, therefore, excellent potential for pharmaceutical uses. The structure of PG-1 in solution as determined by nuclear magnetic resonance (NMR) studies is a one-turn β-hairpin in which two antiparallel strands linked by a β-turn are stabilised by two disulphide bridges [4,5]. The cationic nature of the peptide allows its interaction with the lipid matrix of bacterial membranes containing negatively charged lipids, but its antimicrobial activity itself depends on its ability to form pores in these membranes. Several studies have demonstrated that PG-1 is able to alter the permeability of cellular membranes [6] or of artificial bilayers [7]. Structural investigations by NMR have indicated that this peptide should adopt a dimeric structure in

Abbreviations: CD, circular dichroism; DMF, *N*,*N*-dimethylformamide; DNS-PE, *N*-[5-(dimethylamino)-naphthyl]-1-sulfonyl]dipalmitoyl-L-α-phosphatidylethanolamine; LUVs, large unilamellar vesicles; MALDI-TOF MS, matrix-assisted laser desorption/ionisation time-of-flight mass spectrometry; MLVs, multilamellar vesicles; NBD-PE, *N*-[7-nitrobenz-2-oxo-1,3-diazol-4-yl]dipalmitoyl]-L-α-phosphatidylethanolamine; POPC, 1-palmitoyl-2-oleyl-*sn*-glycero-3-phosphocholine; POPG, 1-palmitoyl-2-oleyl-*sn*-glycero-3-phosphoglycerol; P/L, peptide-to-lipid molar ratio; RET, resonance energy transfer; SUVs, small unilamellar vesicles; TMR, 5-(and-6)-carboxytetramethylrhodamine; TFE, 2,2,2-trifluoroethanol

* Corresponding author. Fax: +33-4-6604-8667.
E-mail address: gdrin@syntem.com (G. Drin).

0005-2736/02/$ – see front matter
PII: S0005-2736(01)00447-3

a membrane-mimetic environment supporting a model in which the association of several dimers results in the formation of a pore [8]. In addition, recent work has provided evidence of the existence of two different states of PG-1 in a lipid bilayer, one corresponding to its parallel orientation on the surface of the membrane and the other corresponding to its transmembranal insertion [9,10].

It has been shown previously that disulphide bridges of protegrin are a prerequisite for its pore formation capability [6]. The linearisation of this peptide offered the possibility of designing analogues able to interact with the cell surface but lacking the membrane-disrupting activity. One of these peptides, SynB1, was shown to enhance the uptake of doxorubicin into cultured multidrug-resistant K562 cells [11] and to increase its transport across the blood–brain barrier in mouse and rat [12,13]. Other vectors, belonging to different cell-permeable peptide families, have been developed recently for the intracellular delivery of therapeutic compounds in vitro and in vivo (see for review [14] and references therein). However, questions were raised about their mode of entry into cells, which does not seem to be via classic endocytosis [14]. For several cell-permeable peptides, it was proposed that they cross the lipid matrix of plasma membranes in an energy-independent manner to penetrate into cells [15,16].

We investigated the ability of a fluorescent analogue of PG-1 and of a fluorescent linear analogue to translocate from the outer to the inner leaflet of a membrane. It was demonstrated previously that the antimicrobial peptide tachyplesin I (TA-1), having a secondary structure similar to that of PG-1 [17], is able to form transient anionic-selective pores and to translocate through phospholipid bilayers [18]. This pore formation–translocation mechanism also concerns natural helical peptides such as magainin [19], mellitin [20] and mastoparan-X [21]. However, no data related to the translocation ability of PG-1 have yet been reported.

We demonstrate here by fluorescence spectroscopy that PG-1, but not its linear analogue, crosses the membrane of phospholipidic vesicles. In addition, we show that the translocation ability of PG-1 is coupled to its pore formation capacity and depends on its folding in a β-hairpin. This suggests that protegrin-derived vectors do not spontaneously cross the lipid matrix of plasma membranes to enter into cells.

2. Materials and methods

Fmoc-PAL-PEG-PS (High Load) and 9-fluorenylmethyloxycarbonyl (Fmoc) amino acids were purchased from Perseptive Biosystems (Hamburg, Germany). Other reagents used for peptide synthesis included *N*,*N*′-diisopropylcarbodiimide (DIPCDI, Fluka), 1-hydroxybenzotriazole (HOBT, Perkin Elmer), *N*,*N*-diisopropylethylamine (DIEA, Fluka), benzotriazole-1-yl-oxy-tris-pyrrolidinophosphonium hexafluorophosphate (PyBop, Novabiochem) and dimethylformamide (DMF, Perseptive Biosystems).

The lipid POPC (1-palmitoyl-2-oleyl-*sn*-glycero-3-phosphocholine) and POPG (1-palmitoyl-2-oleyl-*sn*-glycero-3-phosphoglycerol) were obtained from Avanti Polar Lipids (AL, USA). NBD-PE (*N*-[7-nitrobenz-2-oxo-1,3-diazol-4-yl]dipalmitoyl]-L-α-phosphatidylethanolamine), DNS-PE (*N*-[5-(dimethylamino)-naphthyl]-1-sulfonyl]dipalmitoyl-L-α-phosphatidylethanolamine) and calcein were obtained from Molecular Probes (Eugene, OR, USA). Sodium dithionite, 2,2,2-trifluoroethanol (TFE) and sodium dodecyl sulphate (SDS) were supplied by Sigma (St Louis, MO, USA). Sephadex G75 was purchased from Pharmacia Biotech (Uppsala, Sweden).

2.1. Peptide synthesis

The peptides were synthesised according to Fmoc-tBu strategy using an AMS 422 (ABIMED, Germany). After peptide elongation, resin was treated with piperidine (20% in DMF) to deprotect the N-terminus of peptide, washed with DMF and treated with deprotecting mixture to cleave peptides from resin and deprotect the side-chains. The labelling of TMR-peptide was done in DMF by adding 5-(and-6)-carboxytetramethylrhodamine to the amino-terminal free peptide in presence of DIEA (2 eq) and PyBop (1.5 eq). The cyclisation of PG-1 and [12W]PG-1 by disulphide bridges was realised according to the protocol of Tam et al. [22]. Peptide purification was accomplished by reverse phase high performance liquid chromatography (Water-prep LC 40, Water) under TFA 0,01%/acetonitrile gradient

condition. Purification, as assessed by reverse phase analytic chromatography (Beckman Gold equipped with a Diode Array detector), was over 95% for both peptides by the criterion of UV absorbance at 220, 280 and 540 nm when the peptides were labelled with TMR. The molecular masses were validated by MALDI-TOF spectrometry (Voyager Elite, Perseptive Biosystem, UK).

2.2. Vesicle preparation

For preparation of small unilamellar vesicles (SUVs), a lipid film of the desired composition was dried for 3 h and then suspended in buffer (20 mM Tris, 150 mM NaF and 0.1 mM EDTA (pH 7.4)) to give a final concentration between 25 and 30 mM. The suspension was sonicated in ice-cold water for 25 min using a titanium tip ultrasonicator. Titanium and lipid debris were removed by centrifugation at $100\,000 \times g$. Dynamic light-scattering measurements (Brookhaven Instruments, USA) confirmed the existence of a single population of vesicles (more than 95% of mass content) with a mean diameter of 31 ± 1 nm. For preparation of large unilamellar vesicles (LUVs), the lipid suspension in buffer (20 mM Tris, 150 mM NaCl and 1 mM EDTA (pH 7.4)) was freeze-thawed for five cycles and then extruded through polycarbonate filters (0.1 μm pore size) 21 times. The lipid concentration was determined in duplicate by phosphorus analysis as described in [23].

2.3. Peptide binding

Fluorescence measurements were performed in 3-ml quartz cells at 25 ± 0.1°C under constant magnetic stirring using a SLM AB-2 spectrofluorometer (SLM Instruments, Urbana, IL, USA). For recording the emission spectra of peptide, excitation was set at 280 nm. Both excitation and emission band-pass were set at 4 nm. For each measure, the baseline spectra recorded in the absence of peptide were subtracted from the peptide spectra.

2.4. Dye release

Dye-entrapped LUVs were prepared with a lipid film of desired composition by the use of 70 mM calcein in buffer (pH was adjusted to 7.4 with 1 M NaOH) as a hydrating solution. Calcein-entrapped vesicles were separated from free calcein on a Sephadex-G75 column (18×1 cm). The release of calcein from LUVs was monitored by fluorescence at an emission wavelength of 520 nm (excitation wavelength of 490 nm). The maximum fluorescence intensity corresponding to 100% leakage was determined by the addition of 10 μl of 10% w/v Triton X-100 to 3 ml of the sample. The apparent percent leakage value was calculated according to $100 \times (F - F_0)/(F_{max} - F_0)$. F and F_{max} correspond respectively to the fluorescence intensity before and after the detergent addition. F_0 represents the fluorescence of the intact vesicles. The temperature was monitored at 25 ± 0.1°C.

2.5. Measurement of translocation

Symmetrically labelled LUVs were prepared by hydrating the lipid film composed of POPC, POPG and DNS-PE (70:15:15 mol/mol/mol). The observation of the fluorescence intensity of the Trp residue (328 or 335 nm) upon excitation at 280 nm allows to monitor the resonance energy transfer (RET) from the Trp residue of the peptide to the dansyl fluorophore in the membrane. The temperature was controlled at 25 ± 0.1°C.

2.6. Dithionite ion permeability

A lipid film composed of POPC/POPG/NBD-PE (7:3:0.05 mol/mol/mol) was resuspended with the buffer and freeze-thawed for five cycles. Small aliquots of the multilamellar vesicles (MLVs) were added to the buffer (control) or injected into a peptide solution in the presence of 10 mM sodium dithionite (freshly prepared at 1 M in 1 M Tris, pH 8.8). The fluorescence intensity of NBD at 530 nm (excited at 450 nm) was monitored at 25 ± 0.1°C.

2.7. Circular dichroism (CD) measurement

Peptide CD spectra were obtained on a Jobin Yvon CD6 spectropolarimeter. The spectra were scanned at room temperature in a quartz optical cell of 0.02 cm path length. Baseline spectra for each solvent or vesicle suspension were obtained prior to the peptide spectra. Each peptide was at a

PG-1: H_2N-RGGRLCYCRRRFCVCVGR-$CONH_2$

[12W]PG-1: H_2N-RGGRLCYCRRR**W**CVCVGR-$CONH_2$

PG-AL: H_2N-RGGRL**A**Y**L**RRR**WA**V**L**VGR-$CONH_2$

SynB1: H_2N-RGGRL**S**Y**S**RRRF**STST**GR-$CONH_2$

Fig. 1. Primary sequence of PG-1, [12W]PG-1, PG-AL and SynB1.

concentration of 75×10^{-6} M in buffer (150 mM NaF, 20 mM Tris, 0.1 mM EDTA), in TFE/buffer mixture (v/v 1:1) or in presence of SDS (0.5%). To measure spectra with SUVs, the concentration of peptide was decreased to 50×10^{-6} M^{-1} to ensure complete saturation of peptides with SUVs and to reduce the absorption and diffusion caused by the presence of phospholipid vesicles. When the peptide adopted a preferential helical structure, the helical content was determined from the mean residue ellipticity $[\Theta]$ at 222 nm according to the relation

$$[\Theta]_{222} = -30300[\alpha]-2340$$

where $[\alpha]$ is the amount of helix [24].

2.8. Flow cytometry of cell-association of peptide

K562 cells were cultured in RPMI supplemented with 10% foetal bovine serum. Cells were diluted at 0.3×10^6 cells ml^{-1} 1 day before the experiment. Cell association was measured by flow cytometry using a FACSCalibur (Becton Dickinson, USA). TMR-labelled peptides (1 μM) were incubated with K562 cells (5×10^5 cells per ml) in Opti-MEM medium at 37°C for various periods of time (final volume was 0.5 ml). Thereafter, the cells were washed twice and then resuspended in 0.5 ml of ice-cold PBS for FACS analysis. Cell-associated fluorophores were excited at 488 nm and the fluorescence of TMR was measured at 575 nm. A histogram of fluorescence intensity per cell (1×10^4) was obtained and the calculated mean of this distribution was considered as representative of the amount of cell-associated peptides.

3. Results

3.1. Design and secondary structure of peptides

To measure the interaction of native PG-1 with phospholipidic vesicles and its translocation ability, we synthesised a fluorescent analogue termed [12W]PG-1 (Fig. 1). This peptide corresponds to PG-1 in which an aromatic residue (Phe) located at position 12 was substituted by a similar but fluorescent residue (Trp). We then designed a linear analogue named PG-AL deriving from [12W]PG-1 by substituting all Cys residues involved in disulphide bridges by either alanine or leucine. These residues (Ala at position 6 and 13, Leu at position 8 and 15) were carefully chosen in order to have a linear analogue of [12W]PG-1 with a similar theoretical hydrophobicity. For both peptides, we have calculated the mean residue hydrophobicity $\langle H\rangle$ according to Eisenberg et al. [25] and using the hydrophobicity scale of Wimley and White [26]. The PG-AL associated to a calculated $\langle H\rangle$ value equal to 0.52 is theoretically slightly more hydrophobic than [12W]PG-1

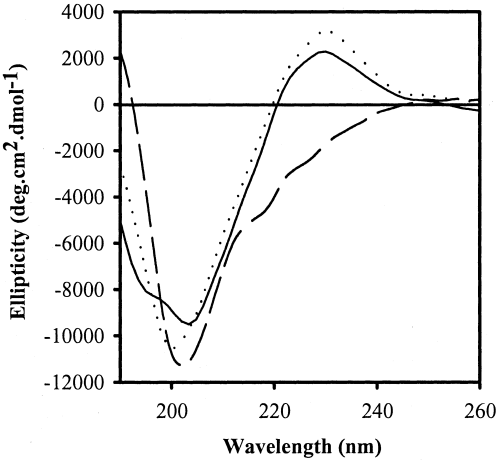

Fig. 2. CD spectra of PG-1, [12W]PG-1 and PG-AL peptides in buffer. Each peptide was used at a concentration of 75 μM in buffer (20 mM Tris, 150 mM NaF, 0.1 mM EDTA, pH 7.4). Solid line, PG-1; dotted line, [12W]PG-1; dashed line, PG-AL.

($\langle H \rangle = 0.47$). The reference peptide SynB1 is associated to a $\langle H \rangle$ value equal to 0.33.

We checked the secondary structure of [12W]PG-1 by recording its CD spectrum as well as that of PG-1 in buffer. The spectrum of both peptides showed a minimum around 200 nm and a maximum at 230 nm (Fig. 2), characteristic of a β-hairpin structure [9]. The slight difference in conformation and/or CD contribution of different aromatic groups in PG-1 and [12W]PG-1 could explain the small difference in curve intensities and shapes observed between the two spectra [27]. As expected, the PG-AL peptide adopts a random coil conformation as indicated by its CD spectrum that exhibited a minimum at 198 nm (Fig. 2).

3.2. Cell uptake of peptides

We incubated the fluorescent TMR-peptides with K562 cells at 1 μM for various times at 37°C to measure the kinetics of cell uptake of peptide by flow cytometry. Fig. 3 shows that the kinetics of cell-uptake of linear peptides SynB1 and PG-AL reach a plateau after 1 h and indicate that PG-AL is better internalised than SynB1. The cell uptake of [12W]PG-1 was somewhat different since it did not reach a final plateau, even after 2 h. In addition, we observed that a large number of cells becoming non-viable after incubation with high concentrations (3 μM) of this cyclised peptide.

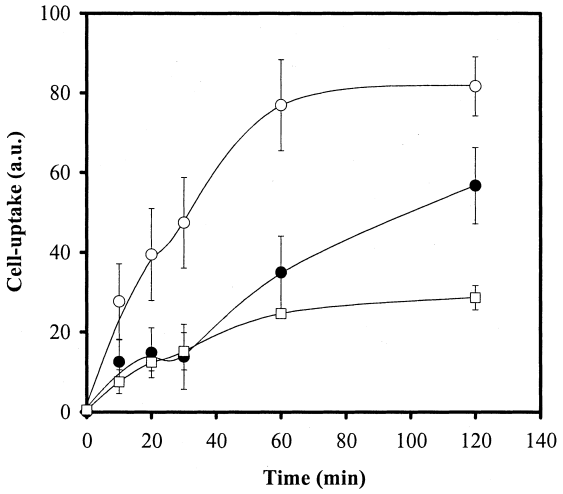

Fig. 3. Cell uptake of peptides into K562 cells. Each TMR-peptide was incubated with K562 cells at 1 μM in Opti-MEM for various times at 37°C. Each value represents the average of triplicate experiments. Error bars correspond to ±S.D. (□) TMR-SynB1, (○) TMR-PG-AL, (●) TMR-[12W]PG-1.

3.3. Peptide interaction

The change of Trp fluorescence emission spectra upon binding to phospholipid vesicles has been widely used to demonstrate the interaction of peptides with phospholipids [27,28]. Fig. 4A,B show, for both peptides, a blue-shift of the wavelength of maximum fluorescence emission when POPC/POPG (70:30 mol/mol) LUVs were added to the peptide solution, indicating that both peptides interacted

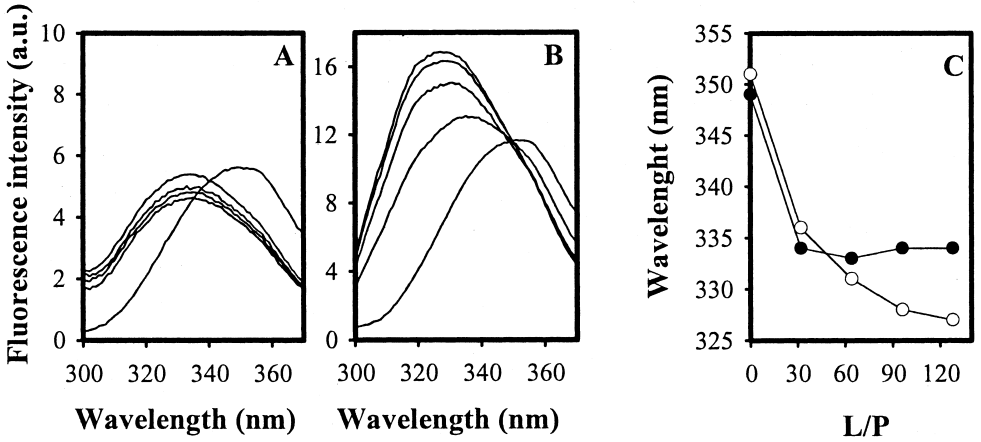

Fig. 4. Interaction of peptides with phospholipidic vesicles. Fluorescence emission spectra of [12W]PG-1 (A) and PG-AL peptide (B) were recorded (excitation at 280 nm) in the absence or presence of 32, 64, 96 or 128 μM LUVs (POPC/POPG 70:30 mol/mol). The peptide concentration was 1 μM. (C) Wavelength of the maximum fluorescence intensity emission represented as function of the lipid-to-peptide molar ratio. (●) [12W]PG-1, (○) PG-AL.

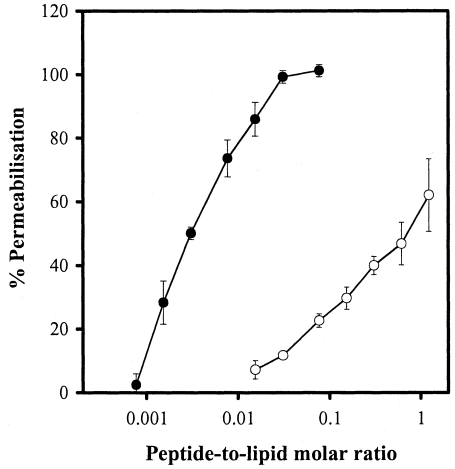

Fig. 5. Membrane-permeabilising activity of [12W]PG-1 and PG-AL peptide. The leakage of calcein entrapped into LUVs (POPC/POPG 70:30 mol/mol) was measured 5 min after addition of [12W]PG-1 (●) or PG-AL (○). The apparent percent leakage value (% permeabilisation) was plotted against the peptide-to-lipid molar ratio. Each value represents the average of triplicate experiments. Error bars correspond to ± S.D.

with the membranes. We have plotted the wavelength corresponding to the maximum fluorescence intensity of Trp residue as function of the lipid-to-peptide molar ratio (Fig. 4C) to indicate that a major fraction of [12W]PG-1 and PG-AL peptides was in a lipid-bound form at a L/P value of 60 and 130, respectively. It should be noted that the blue-shift observed with [12W]PG-1 is accompanied by a decrease in the fluorescence intensity of Trp residue. In contrast, the fluorescence intensity of PG-AL peptide increases upon binding to vesicles.

3.4. Permeabilisation

A dye release assay was performed to examine the membrane permeabilising activity of both peptides. It was measured by an increase in fluorescence intensity due to relief from the self-quenching of calcein concentrated (70 mM) within the LUVs (data not shown). The relationship between apparent percent leakage value and the peptide-to-lipid molar ratio is reported in Fig. 5 and shows that [12W]PG-1 induces

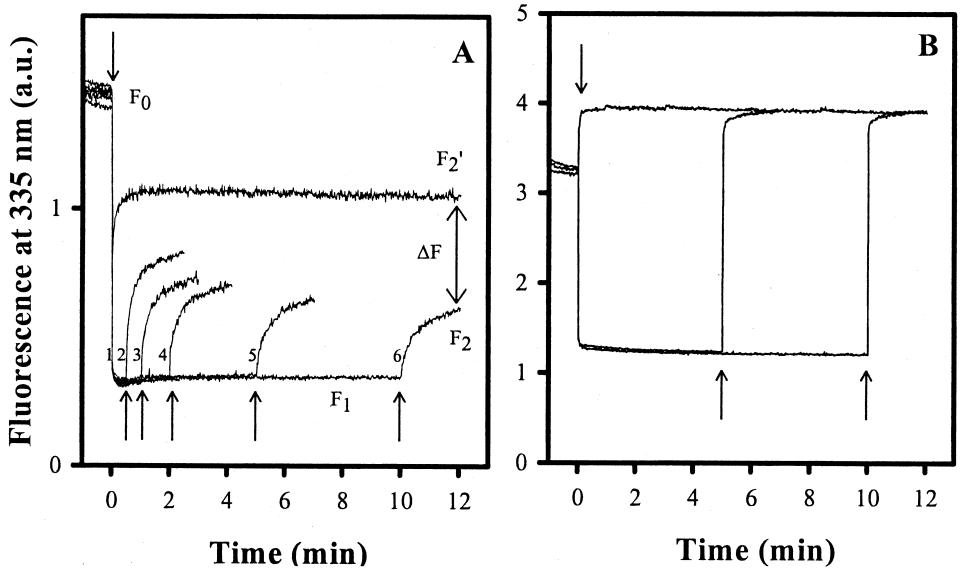

Fig. 6. Detection of the peptide translocation. The peptides [12W]PG-1 (A) and PG-AL (B) were mixed with dansyl-LUVs (POPC/POPG/DNS-PE 70:20:10) at time zero. The peptide and lipid concentrations were 1 and 115 μM, respectively. The fluorescence of Trp at 335 nm (excitation at 280 nm) was recorded. The peptide binding to the vesicles is reflected by the decrease of the intensity from F_0 to F_1 due to RET. At various incubation times (30 s, 1, 2, 5, 10 min, traces 2–6), a large excess (final concentration 730 μM) of a second population of dansyl-free LUVs (POPC/POPG 70:30) was added as indicated by the arrows. An increase in intensity indicates the relief from RET caused by the redistribution between the two vesicle populations of the peptide molecules which had been bound to the outer surface of the first vesicle. The difference (as labelled by ΔF) between final fluorescence intensity (F_2) and the fluorescence intensity (F_2') when both populations of vesicles were simultaneously added at time zero indicates the fraction of peptide which has translocated into the inner leaflet during the incubation time. The trace is representative of five independent measurements.

a leakage of calcein from vesicles at very low peptide-to-lipid molar ratio. In contrast, PG-AL only permeabilises the membranes effectively at very high P/L values.

3.5. Peptide translocation

The translocation was detected according to the protocol described by Matsuzaki et al. [18–21] based on the evaluation of the amount of untranslocated peptides remaining in the outer leaflet of the membranes. The untranslocated peptides can be readily removed from the vesicle surface by extraction with a large excess of a second population of vesicles. The resonance energy transfer (RET) from the Trp residue of the peptide to the dansyl chromophore (DNS-PE) incorporated into the membrane of the first population of vesicles allows determination of the unremovable (i.e., translocated) fraction. At time zero, when dansyl-labelled vesicles (115 μM) were added to a peptide solution (1 μM), a decrease in Trp fluorescence was seen indicating RET due to peptide binding to the membrane (Fig. 6A). After 1 min of incubation, a second population of dansyl-free vesicles (DNS-PE was substituted by POPG) was added in large excess (more than 5-fold). The peptide molecules, which had been bound to the outer leaflet, were redistributed between the two vesicle populations, resulting in a relief from RET and in a fast increase in the fluorescence intensity. In the case of [12W]PG-1, the increased fluorescence intensity was, however, smaller than the intensity obtained when both vesicle populations were simultaneously added to the peptide solution at time zero (as indicated by ΔF). In addition, the final fluorescence decreased with the incubation time, suggesting that a fraction of the peptides became progressively unexposed to the outer leaflet and therefore untransferable to the second vesicles. This indicates a time-dependent peptide translocation. It should be noted that the slow increase of fluorescence observed after addition of the second vesicle population could be attributed to the cross-back of peptides through the membrane of the first vesicle population [18,19,21]. The translocation assay performed with PG-AL showed that no change of fluorescence was observed as a function of time (Fig. 6B). This indicates that PG-AL remains on the outer leaflet of the first population of vesicles and does not translocate through the phospholipid bilayer.

The [12W]PG-1 peptide is entirely protected from the enzymatic action of trypsin as measured by RET at 510 nm in presence of DNS-PE containing vesicles (data not shown). This protection against trypsin treatment, previously observed for tachyplesin I [18], did not allow us to investigate the existence of the [12W]PG-1 translocation through the lipid membrane according to the protocol of Matsuzaki et al. [19,21]. We therefore confirmed the translocation of [12W]PG-1 by using a dithionite-permeability assay [20,21]. Fig. 7 shows that the addition of sodium dithionite, a membrane-impermeable compound, to NBD-PE containing MLVs irreversibly quenches the fluorophore localised on the outermost leaflet (i.e., 15% of the initial NBD fluorescence). The addition of [12W]PG-1 allowed the reducing ion to react with more than 85% of the NBD group within 6 min. If the peptide had permeabilised only the outermost bilayer, the reagent could have reacted with the fluorophore facing the first interlamellar space, resulting in a quenching less than 75% [20,21]. This suggests that the [12W]PG-1 molecule first translocates across

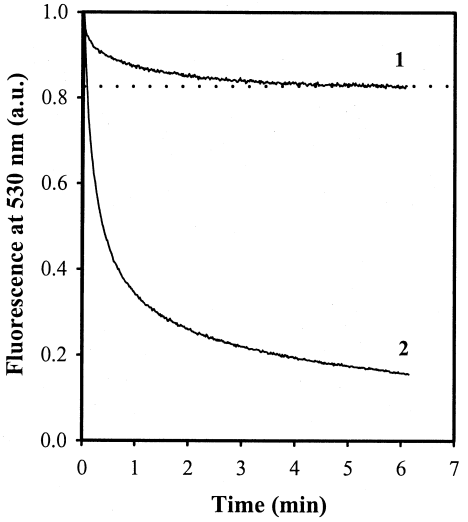

Fig. 7. Detection of [12W]PG-1 translocation. Small aliquots of MLVs composed of POPC/POPG/NBD-PE (70:30:0.5) were added to buffer (trace 1) or to [12W]PG-1 solution (trace 2) in the presence of the 10 mM sodium dithionite. The membrane-impermeant $S_2O_4^{2-}$ quenches irreversibly NBD fluorescence by chemical reduction. The fluorescence at 530 nm (excitation at 450 nm) was normalised to the initial fluorescence in the absence of dithionite. [Lipids] = 42 μM; [Peptide] = 3 μM.

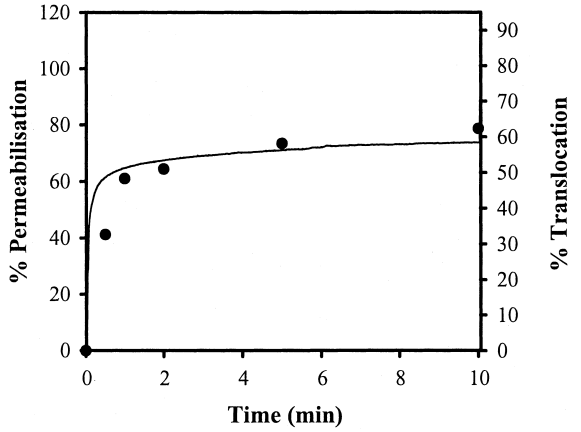

Fig. 8. Relationship between pore formation and peptide translocation for [12W]PG-1. The pore formation was estimated on the basis of the dye release from POPG/POPC (70:30 mol/mol) LUVs (L/P = 115). The peptide and lipid concentration were the same as those for Fig. 6A. The fraction of translocated peptide was evaluated according to $100 \times \Delta F/(F_2' - F1)$ from Fig. 6A.

the outermost bilayer and then destabilises the inner bilayer.

3.6. Correlation between translocation and membrane permeabilisation

Fig. 8 shows a comparison between the kinetics of membrane permeabilisation induced by the [12W]PG-1 and the kinetics of translocation of this peptide determined at the same L/P value of 115. To evaluate the percent translocation value, we used the fluorescence intensity measured 60 s after the addition of dansyl-free vesicles (Fig. 6A). The peptide translocation is coupled with the pore formation estimated from the apparent dye release value, suggesting that [12W]PG-1 crosses the membrane by a pore formation–translocation mechanism.

3.7. Secondary structure of peptides in several environments

CD spectroscopy was used to determine the secondary structure of the peptides in several media. Fig. 9A shows that TFE (50% w/v in buffer) induces a slight modification of the spectrum of the [12W]PG-1 peptide, with a shift of the negative band from 200 towards 203 nm and an increase in the intensity of the signal at 229 nm. This could reflect the modification of the hydrogen-bonding pattern of the peptide in an apolar medium. In the presence of micelles of SDS, there was a slight displacement of the negative band from 200 towards 205 nm, a slight displacement of the positive band at 229 nm and the appearance of a positive band at 190 nm. These modifications are compatible with an increase in the β-sheet content of [12W]PG-1. Finally, in the

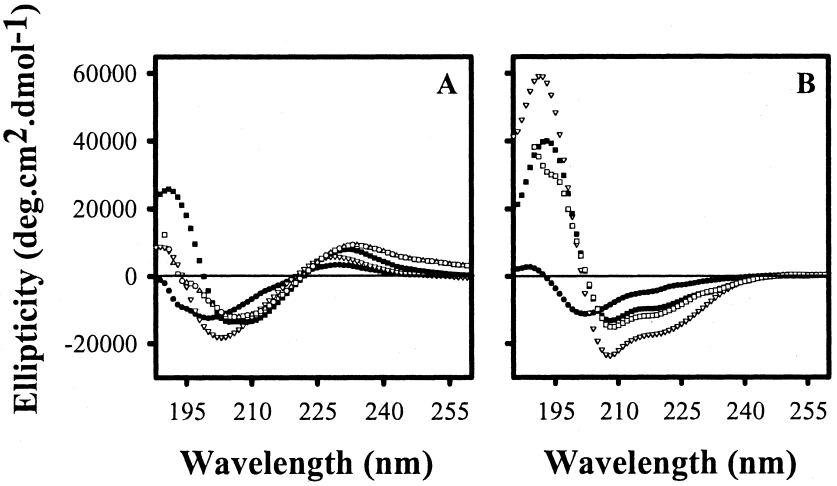

Fig. 9. CD spectra of [12W]PG-1 (A) and PG-AL (B) peptides in different media. CD spectra (●) in buffer (20 mM Tris, 150 mM NaF, 0.1 mM EDTA, pH 7.4), (▽) in TFE (v/v 1:1) 50%, (■) in the presence of SDS micelles at a SDS-to-peptide molar ratio value of 150 with a peptide concentration at 150 μM, and (□) in the presence of POPC/POPG (70:30 mol/mol) SUVs with an L/P value of 160 (the peptide and lipid concentration were equal to 50 μM and 16.3 mM, respectively).

presence of POPC/POPG (70:30 mol/mol) SUVs, we report changes of the CD spectrum similar to those observed in the presence of SDS. As indicated previously in Fig. 2, the PG-AL peptide has no ordered secondary structure in buffer. In the presence of TFE, the CD spectrum of peptide showed minima at 208 and 222 nm and a maximum at 193 nm, characteristic of a right-handed α-helical conformation (Fig. 9B). From the ellipticity value at 222 nm (see Section 2), we evaluated the helical content of peptide to 45.4%. We have also investigated the secondary structure of the peptide in the presence of SDS micelles or upon binding to lipid vesicles and we show that it adopts preferentially a helical conformation with, respectively, a helical content of 21% and 26% (Fig. 9B).

4. Discussion

We have investigated whether protegrin (in a fluorescent form) and a linear analogue PG-AL are able to pass across a lipid bilayer. This study allows us to better understand the relationship between the folding of protegrin and its permeabilisation mechanism upon binding to lipidic membranes. In addition, this study has provided information about the mode of cell uptake of SynB peptides derived from PG-1 by linearisation [11]. It has been previously proposed that the cell uptake of peptides such as penetratin or transportan occurs by crossing the lipid matrix of plasma membranes in an energy-independent manner [29,30]. Thus, our studies allow us to evaluate whether the cell uptake of peptides derived by linearisation of protegrin depends on their translocation through the lipid matrix of the plasma membrane.

We have synthesised a fluorescent analogue of protegrin PG-1, named [12W]PG-1, following the synthesis protocol used previously to produce the protegrin [4,6]. The substitution of residue Phe by Trp at position 12 within the primary sequence does not affect the formation of the β-hairpin turn and disulphide bridge formation, as indicated by the similarity between the CD spectra recorded for PG-1 and [12W]PG-1. The spectra obtained were similar to those reported earlier for native PG-1 [9]. As expected, the PG-AL peptide, a linear analogue of [12W]PG-1, has no defined secondary structure, confirming that the two disulphide bridges are crucial for stabilising the protegrin folding.

By using flow cytometry, we have compared the internalisation of PG-AL and [12W]PG-1 into K562 cells to our reference peptide SynB1 [11–13]. The cell-uptake of PG-AL and SynB1 exhibits a similar kinetic profile, whereas that of [12W]PG-1 is different. This result indicates first that PG-AL is representative of the SynB family in term of cell-uptake and suggests that the linear and cyclised peptides enter into cells by a different mechanism. This was illustrated by the observation made during internalisation assay indicating that only the [12W]PG-1 induced cell death when its concentration was slightly increased (data not shown). Therefore, it is very difficult to compare the internalisation of PG-AL and [12W]PG-1 since for this latter peptide, cell viability might be affected. At opposite, we propose that the strong internalisation of PG-AL compared to those of SynB1 could be due to its higher hydrophobicity, since we have demonstrated that this physico-chemical property could govern the cell uptake of linear peptidic vectors [31].

We have studied the interaction of [12W]PG-1 and PG-AL with membranes containing 30% (mol/mol) negatively charged phospholipids. The interaction of both peptides with the lipid bilayers was monitored by the blue-shift in Trp fluorescence emission spectra due to the re-localisation of this residue from a polar to a hydrophobic environment. The interaction between [12W]PG-1 and lipids was strong as indicated by the low L/P for which we observed a complete saturation of peptide by vesicles. Compared to [12W]PG-1, the PG-AL peptide seems to have a lower lipid-binding affinity, suggesting that the folding of protegrin favours its interaction with phospholipids.

Using a dye release assay, we have shown that [12W]PG-1 induces permeabilisation of membranes at high lipid-to-peptide molar ratio (L/P = 125 for 75% permeabilisation) consistent with a permeabilising mechanism involving the formation of pores [6,7]. Circular dichroism spectra suggest that the β-sheet content of [12W]PG-1 increases upon binding to phospholipid vesicles or in the presence of SDS micelles. This observation agrees with ^{1}H NMR results reported by Roumestand et al. [8] who pro-

posed previously that PG-1 in dodecylphosphocholine micelles is better structured than in water. Thus, the formation of a multimeric pore could depend on the slight rearrangement of the β-hairpin structure of protegrin. In addition, an unusual quenching of Trp fluorescence was observed when the peptides interacted with lipids. One explanation could be that this quenching is due to the close contact between the Trp residue of a [12W]PG-1 monomer and an amino acid belonging to a second one.

The linear analogue of [12W]PG-1 probably does not form pores, as indicated by its low permeabilising activity observed at low lipid-to-peptide molar ratios. In addition, cytotoxicity assays carried out with K562 cells incubated with peptides for 48 h (Mazel et al., unpublished data) indicate that the PG-AL peptide is 4-fold less cytotoxic than [12W]PG-1 and PG-1 (these latter two peptides have the same cytotoxicity). This could reflect the fact that PG-AL has a lower permeabilising potential against natural membranes than [12W]PG-1.

We have assayed the translocation of [12W]PG-1 according to the protocol previously described by Matsuzaki et al. [18–21]. We report here that [12W]PG-1 translocates rapidly from the outer to the inner leaflet of phospholipid bilayer at a high lipid-to-peptide molar ratio. In contrast, the PG-AL peptide does not cross the membrane indicating that the linearisation of [12W]PG-1 suppresses its permeabilising potency as well as its ability to translocate through a lipid bilayer. This agrees with previous observations demonstrating that a linear analogue of tachyplesin, forming a β-sheet at the surface of the phospholipidic bilayer, is not able to pass across membranes [18]. In our study, circular dichroism indicates that, although PG-AL adopts a partial helical conformation in an α-helical promoting medium such as TFE, it has no predominant conformation in a membrane-mimetic environment or upon binding to lipid vesicles. The folding of the protegrin in a β-hairpin, stabilised by disulphide bridges, seems to be a clear determinant for its ability to cross phospholipid membranes.

The translocation of [12W]PG-1 is coupled to its permeabilisation activity, suggesting that protegrin is redistributed between the two leaflets after the formation of a transient pore in the membrane. It should be noted that the translocation observed for [12W]PG-1 and previously for TA-1 [18] occurs at a similar L/P value in the presence of vesicles having a similar phospholipid composition. In addition, the dynamic behaviour of protegrin during pore formation and pore deactivation is consistent with the coexistence of two states of protegrin in the phospholipid bilayer corresponding to a surface-absorbed state and a membrane-spanning state [9]. Moreover, recent X-ray diffraction studies have suggested that protegrin forms a toroidal pore in the membrane [32]. The peptide magainin has also been shown to form toroidal pores, i.e., a multimeric organisation constituted by heads of lipids and peptides localised at the lipid/water interface [33]. In this model, the leaflets of the bilayer fold over onto each other, producing a pore which looks like the inside of a torus lined with peptides ('wormhole' model). It was clearly demonstrated that magainins are able to translocate across membranes [19,34]. Thus, our data support the view that PG-1 interacts with and translocates through the lipid membranes following the 'wormhole' model.

The membrane permeabilisation mechanism of protegrin seems to correspond to the model proposed for tachyplesin and other peptides by Matsuzaki [34]. We demonstrate that this property of PG-1 depends on its secondary structure, meaning that the linear analogues derived from this peptide cannot spontaneously cross a lipid membrane. Thus, we propose that the linearisation of PG-1 generates peptidic vectors which are able to interact with the cellular membranes but which cannot pass through their lipidic matrix. The results obtained by the internalisation assays suggest that the linear and disulfide bridged analogues of PG-1 have a different mode of cell uptake. Therefore, this could mean that the penetration of these linear peptides into intact cells depends on an energy-dependant pathway. A recent work supports this view by indicating that the internalisation of SynB1 into the endothelial cells of the blood–brain barrier may involve adsorptive mediated endocytosis [13]. However, we cannot exclude the possibility that the cell uptake of SynB peptides involves, in part, an unexplained energy-independent pathway, as observed for other cationic peptidic vectors [35]. Our continuing studies are aimed at better understanding the cellular import of linear analogues of protegrin.

Acknowledgements

We thank Professor Robert Brasseur, Professor Anthony Rees and Dr P. Clair for their advice and critical evaluations of the manuscript. We acknowledge M. Mazel and P. Merida for the flow cytometry and cytotoxicity assay. We are indebted to Dr F. Roux and M. Paolini for peptide synthesis and purification, Dr J. Sainte-Marie for help with phosphorus analysis, Dr C. Braud for use of a circular dichroism spectropolarimeter, and Dr M. Jullien for use of a photon correlation spectrometer. This work was supported by a grant from ANRT (Association Nationale pour la Recherche et la Technologie) to G.D.

References

[1] V.N. Kokryakov, S.S. Harwig, E.A. Panyutich, A.A. Shevchenko, G.M. Aleshina, O.V. Shamova, H.A. Korneva, R.I. Lehrer, FEBS Lett. 327 (1993) 231–236.
[2] X.D. Qu, S.S. Harwig, A.M. Oren, W.M. Shafer, R.I. Lehrer, Infect. Immun. 64 (1996) 1240–1245.
[3] B. Yasin, R.I. Lehrer, S.S. Harwig, E.A. Wagar, Infect. Immun. 64 (1996) 4863–4866.
[4] A. Aumelas, M. Mangoni, C. Roumestand, L. Chiche, E. Despaux, G. Grassy, B. Calas, A. Chavanieu, Eur. J. Biol. Chem. 237 (1996) 575–583.
[5] R.L. Fahrner, T. Dieckmann, S.S. Harwig, R.I. Lehrer, D. Eisenberg, J. Feigon, Chem. Biol. 3 (1996) 543–550.
[6] M.E. Mangoni, A. Aumelas, P. Charnet, C. Roumestand, L. Chiche, E. Despaux, G. Grassy, B. Calas, A. Chavanieu, FEBS Lett. 383 (1996) 93–98.
[7] Y. Sokolov, T. Mirzabekov, D.W. Martin, R.I. Lehrer, B.L. Kagan, Biochim. Biophys. Acta 1420 (1999) 23–29.
[8] C. Roumestand, V. Louis, A. Aumelas, G. Grassy, B. Calas, A. Chavanieu, FEBS Lett. 421 (1998) 263–267.
[9] W.T. Heller, A.J. Waring, R.I. Lehrer, H.W. Huang, Biochemistry 37 (1998) 17331–17338.
[10] W.T. Heller, A.J. Waring, R.I. Lehrer, T.A. Harroun, T.M. Weiss, L. Yang, H.W. Huang, Biochemistry 39 (2000) 139–145.
[11] M. Mazel, P. Clair, C. Rousselle, P. Vidal, J.M. Scherrmann, D. Mathieu, J. Temsamani, Anticancer Drugs. 12 (2001) 107–116.
[12] C. Rousselle, P. Clair, J.M. Lefauconnier, M. Kaczorek, J.M. Scherrmann, J. Temsamani, Mol. Pharmacol. 57 (2000) 679–686.
[13] C. Rousselle, M. Smirnova, P. Clair, J.M. Lefauconnier, A. Chavanieu, B. Calas, J.M. Scherrmann, J. Temsamani, J. Pharmacol. Exp. Ther. 296 (2001) 124–131.
[14] M. Lindgren, M. Hällbrink, A. Prochiantz, U. Langel, Trends Pharmacol. Sci. 21 (2000) 99–103.
[15] J.P. Berlose, O. Convert, D. Derossi, A. Brunissen, G. Chassaing, Eur. J. Biochem. 242 (1996) 372–386.
[16] M. Pooga, M. Hällbrink, M. Zorko, U. Langel, FASEB J. 12 (1998) 67–77.
[17] H. Tamamura, M. Kuroda, M. Masuda, A. Otaka, S. Funakoshi, H. Nakashima, N. Yamamoto, M. Waki, A. Matsumoto, J.M. Lancelin, K. Daisuke, S. Tate, F. Inagaki, N. Fujii, Biochim. Biophys. Acta 1163 (1993) 209–216.
[18] K. Matsuzaki, S. Yoneyama, N. Fujii, K. Miyajima, K. Yamada, Y. Kirino, K. Anzai, Biochemistry 36 (1997) 9799–9806.
[19] K. Matsuzaki, O. Murase, N. Fujii, K. Miyajima, Biochemistry 34 (1995) 6521–6526.
[20] K. Matsuzaki, S. Yoneyama, K. Miyajima, Biophys. J. 73 (1997) 831–838.
[21] K. Matsuzaki, S. Yoneyama, O. Murase, K. Miyajima, Biochemistry 35 (1996) 8450–8456.
[22] J. Tam, C. Wu, W. Liu, J. Zhang, J. Am. Chem. Soc. 113 (1991) 6657–6662.
[23] G.R. Bartlett, J. Biol. Chem. 234 (1959) 466–468.
[24] Y.H. Chen, J.T. Yang, J. Martinez, Biochemistry 11 (1972) 4120–4131.
[25] D. Eisenberg, R.M. Weiss, T.C. Terwilliger, Nature 299 (1982) 371–374.
[26] W.C. Wimley, T.P. Creamer, S.H. White, Biochemistry 35 (1996) 5109–5124.
[27] N.G. Park, S. Lee, O. Oishi, H. Aoyagi, S. Iwanaga, S. Yamashita, M. Ohno, Biochemistry 31 (1992) 12241–12247.
[28] V.K. Mishra, M.N. Palgunachari, Biochemistry 35 (1996) 11210–11220.
[29] J.P. Berlose, O. Convert, D. Derossi, A. Brunissen, G. Chassaing, Eur. J. Biochem. 242 (1996) 372–386.
[30] M. Pooga, M. Hällbrink, M. Zorko, U. Langel, FASEB J. 12 (1998) 67–77.
[31] G. Drin, M. Mazel, P. Clair, D. Mathieu, M. Kaczorek, J. Temsamani, Eur. J. Biochem. 268 (2001) 1304–1314.
[32] L. Yang, T.M. Weiss, R.I. Lehrer, H.W. Huang, Biophys. J. 79 (2000) 2002–2009.
[33] S.J. Ludtke, K. He, W.T. Heller, T.A. Harroun, L. Yang, H.W. Huang, Biochemistry 35 (1996) 13723–13728.
[34] K. Matsuzaki, Biochim. Biophys. Acta 1462 (1999) 1–10.
[35] A. Scheller, J. Oehlke, B. Wiesner, M. Dathe, E. Krause, M. Beyermann, M. Melzig, M. Bienert, J. Pept. Sci. 5 (1999) 185–194.